16th World Conference on Earthquake, 16WCEE 2017
Santiago Chile, January 9th to 13th 2017
Paper N° 1284 (Abstract ID)
Registration Code: S-Z1462947012

FORCE-BASED BEAM-COLUMN ELEMENT WITH MULTISPRING MODELS FOR MODELLING POST-TENSIONED ROCKING MEMBERS

C.-L. Lee[(1)]

[(1)] *Senior Lecturer, University of Canterbury, Christchurch, New Zealand, chin-long.lee@canterbury.ac.nz*

Abstract

Post-tensioned rocking beams and columns are popularly used in earthquake-resistant structures because of their self-centring and low-damage response characteristics. Rocking actions in these members arise from the open-and-close action at their two end joints. A post-tensioned prestressing tendon passing through the members and the joints provides the axial and moment continuity between the members and the joints. Rocking at member interior joints may also be provided for segmental rocking members, which are usually used as bridge piers. Because the plane sections of the rocking members at the joints do not remain plane during the rocking action, the traditional beam-column finite elements based on classical plane-section beam theories are no longer applicable to simulate the rocking motions. As a result, a new type of beam-column finite element is needed. In this paper, a new rocking beam-column element is proposed. The new element allows multiple rocking joints to be anywhere within the beam-column members, and, therefore, is applicable to both traditional end rocking members and segmental rocking members. It is derived based on the mixed formulation that interpolates the force field exactly but satisfies the strain-displacement compatibility weakly. The formulation allows the relaxation of plane-section assumption at the rocking joints using the idea of multispring models. The new element can be readily used to simulate the seismic response of a large-scale structures with multiple rocking beams and columns. The new element accurately simulates the experimental results of a rocking column undergone a series of bi-axial loading. To demonstrate its advantages in large-scale simulations, the new element is also used to model the dynamic response of a large-scale structure. The results indicate that this new element shows highly promising potentials for large-scale structural analysis.

Keywords: rocking member; self-centring; beam-column element; multispring; unbonded post-tensioned

1. Introduction

Rocking columns have recently become popularly used in earthquake-resistant design because of their self-centering force-displacement response characteristics that could minimize the permanent residual displacement of a structure after an earthquake event [1–3]. Often times, with a nearly elastic response, rocking columns also result in little or controllable damage in their components during earthquakes. Numerical modeling of rocking columns then becomes important to characterize their seismic performance in bridges and multi-story buildings.

Numerical modeling of rocking columns in a large-scale structure is, however, challenging when, in particular, a compromise between two competing simulation requirements, computational efficiency and response accuracy, is unavoidable. The challenge is due to the fact that the response behavior at the rocking interface between columns and joints violates the usual beam theory that assumes plane section remaining plane after deformations. As a result of this violation, a simple lumped plasticity model based on moment-rotation relationship [4, 5], though computationally very efficient, would not be sufficiently accurate to simulate the response, especially for rocking columns subjected to arbitrary loadings and variable axial load. Under these loading scenarios, a finite element model that does not require the beam theory assumption would be accurate. However, the computational efficiency would be drastically reduced and render the model almost infeasible, especially, for a time history analysis of large-scale rocking structures.

In meeting a compromised requirement between computational efficiency and response accuracy, a third type of models is warranted, and that leads to the development of a multispring model [6–8]. The multispring model is a two-node, usually zero length, fiber-like model that has multiple compression-only uniaxial springs connecting its two end nodes. It is used to model the column region near the rocking interface, where the beam theory fails to apply. A linear elastic frame element connected in series is typically used to simulate the remaining region of the column where the beam theory applies.

In the multispring model, the compression-only spring consists of a spring sub-element and a gap sub-element connected in series. The gap sub-element remains closed when the spring sub-element experiences a compressive stress, and opens when the spring sub-element may otherwise experiences a tensile stress. The gap sub-element facilitates the relaxation of the beam theory assumption at the rocking interface, therefore, allows the model to better simulate the strain distribution in the column at the region near the rocking interface.

When compared with the lumped plasticity model and the finite element model, the multispring model is the best candidate to meet the competing needs between efficiency and accuracy. Nevertheless, the determination of the length of the spring sub-elements, which is the characteristic length measuring the length of the zone inside the rocking column where the beam theory does not apply, usually requires calibration from experimental data. While the multispring model is generally accepted as the best option to model the rocking interface, it has the following shortcomings:

1. The spring sub-elements introduce additional flexibility at the rocking interface, so the flexibility of the connecting column element needs to be reduced to avoid changing the overall column flexibility. This change may be straightforward for members with linear elastic materials with certain boundary conditions, but not so for nonlinear materials like concrete. A simple correction of axial stiffness of the connecting column element might also lead to an erroneous recovery of elastic flexibility, as to be shown later.

2. Shear force transfer is missing. Either a displacement constraint or an additional shear transfer component is required. The former adds computational complexity and the latter adds model complexity.

3. Modeling the rocking interface as a tiny element separated from the connecting column element results in combining a high stiffness element (before a gap is opened) and a low stiffness element in the system. Consequently, an ill-conditioned global stiffness matrix is likely formed, which could lead to numerical instability during solution iteration.

The work reported here sets out to overcome the above shortcomings by proposing to incorporate multispring models into column elements, in particular, force-based beam-column elements, which have been demonstrated to be accurate, efficient and robust in modeling members with large deformations [9, 10]. The incorporation will involve modifications of the formulation of force-based beam-column elements. As demonstrated in the following sections, the modification is not simply joining multiple elements with the internal nodes eliminated by static condensation.

The following sections will first give a brief introduction of the multispring model, followed by a discussion on the errors arose from a common practice [7, 11, 12] during calibration, where only a simple correction of the axial stiffness of the elastic frame element connecting to the multispring model is done.

The paper subsequently introduces the force-based beam-column element and its new, modified formulation that incorporates the multispring model as part of the element. The advantages of the new formulation will be highlighted and demonstrated using numerical examples.

The beam-column elements with the new formulations have been implemented in the Matlab toolbox FEDEASLab (http://fedeaslab.berkeley.edu) that allows nonlinear structural simulations under static and transient loading [13], and will soon be implemented in OpenSees (http://opensees.berkeley.edu) [14].

2. Multispring Model and Calibration Problems

A multispring model is essentially a two-node element made of multiple uniaxial spring-gap elements connecting the rigid links stemming out from two end nodes, which are typically coincide in a numerical model with zero distance. The end displacements of each spring element are obtained from the nodal displacements through kinematic compatibility. A schematic diagram of a two-dimensional (2D) multispring model is shown in Fig. 1.

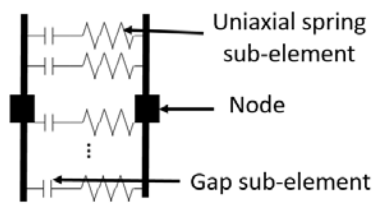

Fig. 1 – Multispring model

The uniaxial spring-gap elements contribute only to the axial force and moment transfer, but not to the shear transfer, between two end nodes. While some transverse or diagonal spring sub-elements may be added to ensure a transfer of transverse shear [15], they are typically not used because their force-displacement constitutive relationships are difficult to be calibrated, especially considering the interaction among axial force, shear force and flexural moments. Hence, a transverse displacement constraint would need to be imposed on the two end nodes to avoid instability.

The multispring model has a non-zero flexibility (inverse of stiffness) even when there is no rocking motion, because a non-zero characteristic length has been used for its spring sub-elements, even though its two end nodes are coincide in the model with zero distance apart. This flexibility would be added to the flexibility of the frame element connected in series to yield the total flexibility of the rocking column. If the flexibility of the frame element, which has the model length equal to the physical length of the rocking column, is obtained based on actual material and section properties of the column material, the total flexibility would be larger than the actual flexibility. To avoid this error, the flexibility of the frame element needs to be reduced by the amount of flexibility of the multispring model.

Correcting the axial flexibility of the connecting element is straightforward, as typically done by many [7, 11, 12]. The axial flexibility of the frame element is simply reduced according to the following:

$$E_c A_c = \frac{EA}{1 - EA/(Lk_a)} \tag{1}$$

where E and A are the material Young's modulus and cross-sectional area of the rocking member, respectively, E_c and A_c are the modified versions of E and A for the connecting elastic member of length L, and k_a is the axial stiffness of the multispring model.

While correcting the axial flexibility may be easy and straightforward, correcting the flexural flexibility is not, and could easily be done wrong. For example, the correction for a 2D case when the multispring model is connected at joint i of the frame element requires the following equation of flexibility (after removing the rigid body modes) be satisfied:

$$\frac{L}{6E_cI_c}\begin{bmatrix} 2 & -1 \\ -1 & 2 \end{bmatrix} + \begin{bmatrix} 1/k_b & 0 \\ 0 & 0 \end{bmatrix} = \frac{L}{6EI}\begin{bmatrix} 2 & -1 \\ -1 & 2 \end{bmatrix} \tag{2}$$

where I and I_c are the second moments of inertia for the original and modified frame element, and k_b is the flexural stiffness of the multispring model.

In this equation, the first diagonal term in the flexibility matrix requires $E_cI_c = EI/(1 - 3EI/(Lk_b))$, while all other terms require $E_cI_c = EI$. If the product E_cI_c is the only parameter one can vary, this is clearly a dilemma that one cannot resolve. This dilemma only becomes a non-issue if the moment at joint j of the element is always zero, since only the equality of the first diagonal needs to be satisfied. This, however, only corresponds to the case of a cantilever column with post-tensioning tendon going through its centroid. In general, correcting flexural stiffness of the frame element would require a direct change in the element stiffness matrix instead of changing only the parameter E_cI_c. In other words, a new formulation for a rocking beam-column element would be needed to combine both multispring model and the connecting frame element as a single element to avoid this problem.

3. Element Formulation

3.1 Mixed formulation of beam-column elements

The basic deformations with the removal of rigid body modes experienced by the multispring model are axial opening and hinge rotations. The corresponding basic forces are axial force and hinge moments. These basic forces and deformations are consistent with the basic section forces and deformations based on the Euler-Bernoulli's assumption. Therefore, the multispring model can be readily incorporated into an Euler-Bernoulli beam-column element, as demonstrated in the following.

This section discusses how multispring models can be incorporated into force-based beam-column elements in consistent with the mixed formulation. It first introduces the key equations of the mixed formulation and follows by explaining how the key equations can be modified to incorporate the multispring models.

A detailed discussion of the derivations and implementation of the mixed formulation has been given in previous works [10, 16-20]. The following gives only a brief explanation of this formulation and highlight the key equations in the formulation.

The following discussion is limited to frame elements based on the Euler-Bernoulli assumption where plane sections remain plane and normal to the element axis after deformation. For ease of illustration, the following derivation is introduced in the context of two-dimensional (2D) space. The same derivation can be extended to the frame element in three-dimensional space by adding relevant components in the third dimension.

The deformations, in the vector $\mathbf{v}$, of a distributed inelasticity frame element (or beam-column elements) in its basic system without considering rigid body modes consist of axial deformation and end rotations. Correspondingly, the basic element forces, in the vector $\mathbf{q}$, consist of axial force and end moments. The forces $\mathbf{q}$ and the deformations $\mathbf{v}$ of a 2D frame element of length L are shown in Fig. 2(a), together with section deformations and forces shown in Fig. 2(b) under the Euler-Bernoulli assumption. The section deformations, in the vector $\mathbf{e}$, consist of the axial strain ε_a at the reference axis and the curvature κ. Correspondingly, the section forces, in the vector $\mathbf{s}$, consist of the axial force N and the bending moment M.

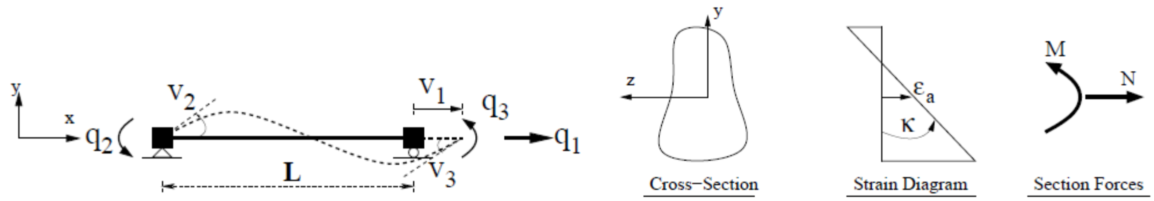

(a) Basic forces and deformations of a 2D frame element

(b) Forces and deformations of a 2D Euler-Bernoulli section

Fig. 2 – Basic forces and deformations for a 2D Euler-Bernoulli beam-column element

In the mixed formulation, the section forces **s** are interpolated from the element forces **q** by satisfying the element equilibrium in the undeformed configuration:

$$\mathbf{s}(\mathbf{q}, x) = \mathbf{b}(x)\mathbf{q} \tag{3}$$

where **b** is the force interpolation matrix. With the interpolation in Eq. (3), the compatibility relationship between the element deformations **v** and the section deformations **e** can be established as shown in the following

$$\mathbf{v} = \int_0^L \mathbf{b}^{\boldsymbol{T}}\mathbf{e}(x)dx \tag{4}$$

The section deformations **e** and the section forces **s** are related through the section constitutive relationship, which can also be derived from material constitutive relationships.

Eqs. (3) and (4) are two key equations in implementing the mixed formulation into the finite element program. Several implementations of the mixed formulation in the finite element program have been discussed extensively in previous works [10, 16, 19, 21].

In the finite element implementation the compatibility relationship in Eq. (4) is evaluated numerically as

$$\mathbf{v} = \sum_{i=1}^{N_p} (\mathbf{b}^{\boldsymbol{T}}\mathbf{e})\,|_{x=\xi_i} w_i \tag{5}$$

where N_p is the number of integration points, ξ_i the integration locations and w_i the weights of the numerical scheme. If little is known a priori about the distribution of **e**, Gauss-Lobatto quadrature would be popularly used in the numerical evaluation because it not only has the highest accuracy with the smallest number of integration points, but also places integration points at the element ends, where the bending moments are largest without element loads. If inelastic section response would only occur at the element ends, with the knowledge of fixed or growing plastic hinge lengths, the modified Gauss-Radau plastic hinge integration method [18] or the MEPI method [20] may offer better accuracy and efficiency.

The numerical weight w_i in Eq. (5) is usually interpreted as the size of the i^{th} region where the integrand $\mathbf{b}^T\mathbf{e}$ is constant. Whenever an inelastic response occurs at i^{th} section, its inelastic or plastic deformations would spread uniformly over the i^{th} region. Hence, the weight w_i can also be interpreted as the *plastic hinge length*.

3.2 Modification of mixed formulation

As discussed previously, the compatibility relationship in Eq. (5) is used to implement the beam-column element based on the mixed formulation, but it is not yet ready for incorporating the multispring model. This expression requires some modifications, as shown in the following.

While the formulation of the force-based beam-column element is traditionally viewed as a formulation for modeling members with distributed inelasticity response, it can be easily modified to incorporate element with concentrated inelasticity hinge joint at any locations, as shown in the following with *n* concentrated inelasticity hinges:

$$\mathbf{v} = \mathbf{f^e q} + \sum_{i=1}^{n} \mathbf{b}_i^T \mathbf{v}_{\mathbf{h}i}^{\mathbf{p}} \tag{6}$$

where $\mathbf{f^e}$ is the elastic element flexibility matrix, and $\mathbf{v_h}^{\mathbf{p}}$ is the plastic deformation of a plastic hinge joint at location ξ_i. In the above expression the subscript i has been used to indicate that the subscripted variable is evaluated at $x = \xi_i$.

The elastic element flexibility matrix can be obtained by integrating elastic section flexibility matrix $\mathbf{f_s}^{\mathbf{e}}$ over the element length, written as

$$\mathbf{f^e} = \int_0^L \mathbf{b}^T(x)\mathbf{f_s^e}(x)\mathbf{b}(x)dx \tag{7}$$

If $\mathbf{f_s}^{\mathbf{e}}$ is uniform throughout the element, a closed-form expression of $\mathbf{f^e}$ can be readily used. Otherwise, either a closed-form expression of $\mathbf{f^e}$ can be derived if $\mathbf{f_s}^{\mathbf{e}}$ can be expressed as a well-defined function of the x-coordinate in the beam axis, or a numerical quadrature may be used to evaluate the integral in Eq. (7) with a desired level of accuracy. In any case, the matrix $\mathbf{f^e}$ usually remains unchanged throughout the course of analysis, and its calculation only needs to be performed once. For a material like concrete, there is no well-defined elastic modulus. A modulus value that could best describe the material response within small deformation regime without losing the desired level of accuracy may be used.

The new expression in Eq. (6) infers that the element deformations $\mathbf{v}$ are the sum of elastic deformation of an elastic member and the contributions from n inelastic hinges at the location $x = \xi_i$ and with the inelastic hinge displacements $\mathbf{v_h}^{\mathbf{p}}$, as depicted in Fig. 3 where a distributed inelasticity element is interpreted as an element with n inelastic hinges connected through linear elastic members.

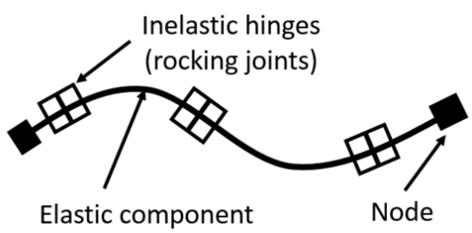

Fig. 3 – An element with elastic component and inelastic hinges (rocking joints)

The inelastic hinges within the element can be directly replaced by the inelastic components of the rocking joints. In most cases rocking joints are implemented in terms of the force-displacement relationship, i.e. $\mathbf{q_h}$-$\mathbf{v_h}$, Eq. (6) may also be written as

$$\mathbf{v} = \mathbf{f^e q} + \sum_{i=1}^{n} \mathbf{b}_i^T (\mathbf{v}_{\mathbf{h}i} - \mathbf{f_h^e q}_{\mathbf{h}i})\mathbf{v}_{\mathbf{h}i}^{\mathbf{p}} \tag{6}$$

where $\mathbf{f_h}^{\mathbf{e}}$ is the elastic flexibility of rocking joints. It is typically equal to the elastic section flexibility $\mathbf{f_s}^{\mathbf{e}}$ multiplied by the characteristic length of the rocking joint.

With the compatibility relationship rewritten as shown in Eqs. (6) and (8), the frame element can now be readily used for modeling rocking columns. The new element has the following advantages not found in the previously derived formulations [16-18, 20], in addition to overcoming the limitations of multi-spring model discussed in the introduction:

1. Rocking hinges can be at any locations within the element.
2. The characteristic lengths of rocking hinges can be of any value based on calibrated data.
3. The linear elastic response can be obtained exactly when no rocking occurs.

4. By keeping some inelastic hinges as non-rocking inelastic joints, this formulation can be applied to nonlinear inelastic RC rocking members

3.3 Modeling tendons and dampers

Rocking columns rely on post-tensioned tendons to have self-centering response and dampers to dissipate energy during a seismic event. The post-tensioned straight tendons in rocking columns can be modeled with a truss element. The feature of element rigid offsets can be used for tendons not passing through the center of the columns. The pre-stressing forces in the rocking column and its tendons would give rise to initial deformations in the elements prior to the application of external loadings. These initial element deformations would need to be implemented to avoid an erroneous force transfer to adjacent elements.

Energy dissipated dampers are often installed at the rocking interface of the columns to allow for some energy to be dissipated during a seismic event. The dampers can be modeled as additional spring elements in the multispring model, except that they also resist tension. Since the dampers are usually installed after the application of the prestressing force, the deformations in the spring elements for modeling dampers should exclude the initial deformations due to the prestressing.

4. Numerical Examples

The performance of the proposed new formulation is evaluated by simulating cyclic responses of a cantilever rocking reinforced concrete (RC) column subjected to bi-axial displacement-controlled loading and a multi-storey post-tensioned timber building subjected to a recorded earthquake ground motion. The first example aims to evaluate the accuracy of the proposed formulation in simulating a rocking RC column experimentally tested. The second example aims to showcase its robust performance in a large-scale structural model. These examples were computed using FEDEASLab [13].

4.1 Cantilever rocking column

This example involves an experimentally tested rocking RC column specimen [22], as shown in Fig. 4. This column, with a cross-section of 350 mm x 350 mm, has 16 reinforcing bars of 10 mm diameter around its inner core. It is post-tensioned with four tendons of 100 mm^2 cross-sectional area going through its center, each with 72 kN initial prestressing force. Eight energy dissipating devices of 8 mm diameter and 115 mm fuse length are connected at the column base with two at each column face. The column is loaded laterally at its top end with a displacement history following a cloverleaf pattern with increasing amplitudes.

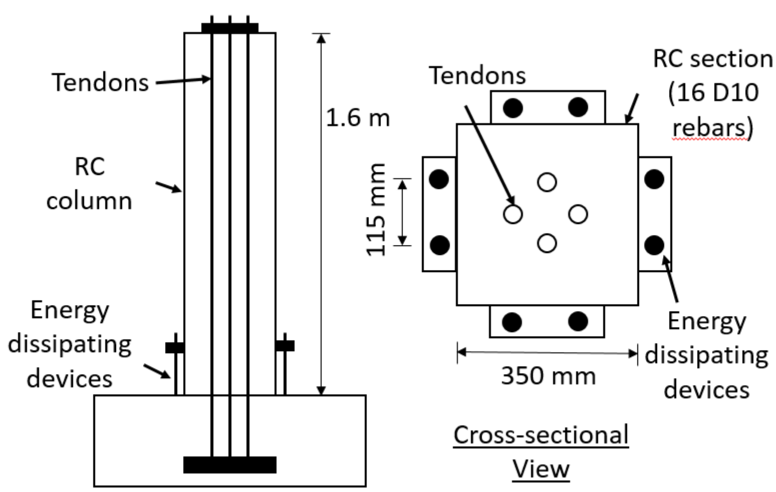

Fig. 4 – The geometry of the post-tensioned RC column

In the numerical model, the column is modeled with one single beam-column element, with the rocking interface incorporated as an internal rocking hinge based on multispring model. The tendons are each modeled with one single truss element with rigid offset. The energy dissipating devices are each modeled with a single spring element incorporated as part of the rocking hinge in the column element. Prestressing forces in the column and tendons are converted as initial deformations in the elements.

The constitutive models used for the concrete and steel (including reinforcement and energy dissipating devices) are the Mander model [23] and Menegotto-Pinto (GMP) model [24] modified by Filippou [25]. The steel tendon is modeled as linear elastic. For the concrete material model, the compressive strength at 28 days is 49.5 MPa, the strain at maximum strength is 0.002, and the confinement ratio is 1.5. For the steel reinforcing material model, the Youngs modulus is 193 GPa, the yield strength is 320 MPa, and the strain hardening ratio is 2%. For the steel energy dissipating devices, the Youngs modulus is 200 GPa, the yield strength is 300 MPa, and the strain hardening ratio is 2%. For the steel tendon material model, the Youngs modulus is 197 GPa.

For the internal rocking hinge of the beam-column element, the concrete material is modeled with 8 x 8 number of compression-only fibers. Each steel reinforcement is also modeled with a compression-only spring. The characteristic length is equal to the width of the cross-section.

Fig. 5 compares the numerical results against experimental results in terms of the lateral resisting force time histories at the column top, which show very good agreement throughout the loading cycles, except for the first few series. This discrepancy could be attributed to the limitations of constitutive models in modeling the energy dissipating devices, and can be resolved with better calibrations. The characteristic length could be another parameter that needs fine-tuning as well. Nevertheless, overall, these comparisons have demonstrated a remarkable accuracy of the proposed beam-column element.

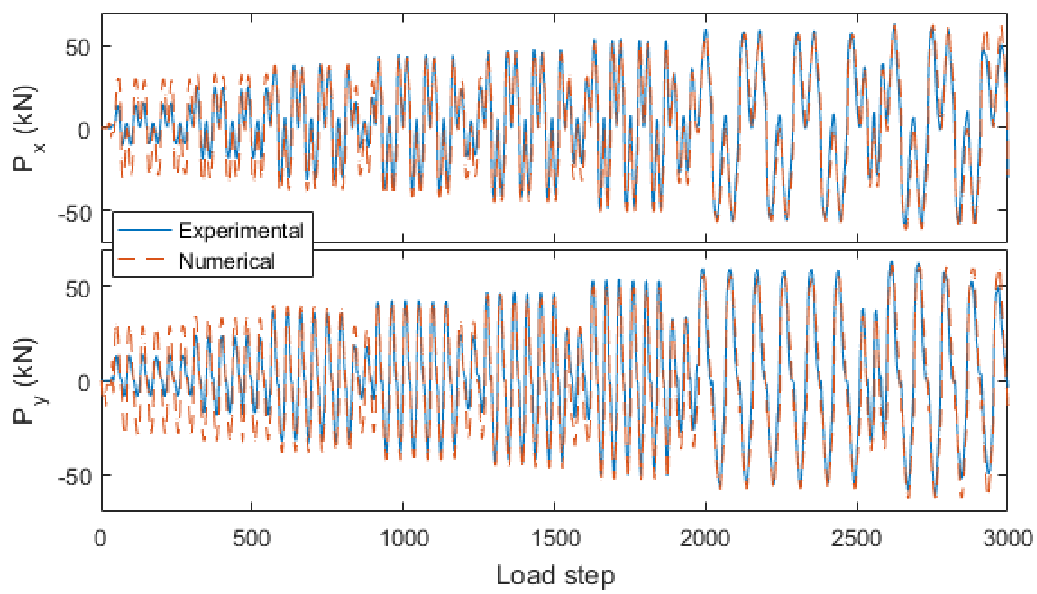

Fig. 5 – Comparison between numerical and experimental lateral resisting force time histories for the post-tensioned RC column

4.2 Multi-storey timber frame

In this example, the proposed beam-column is used to simulate a two-dimensional, 1-bay, 3-storey, post-tensioned timber frame made of two columns and three post-tensioned beams (see Fig. 6), which was slightly modified from the timber frame experimentally tested [26]. The experimental results, however, will not be used for comparison, as the main purpose in this example is only to demonstrate the robustness of the element performance.

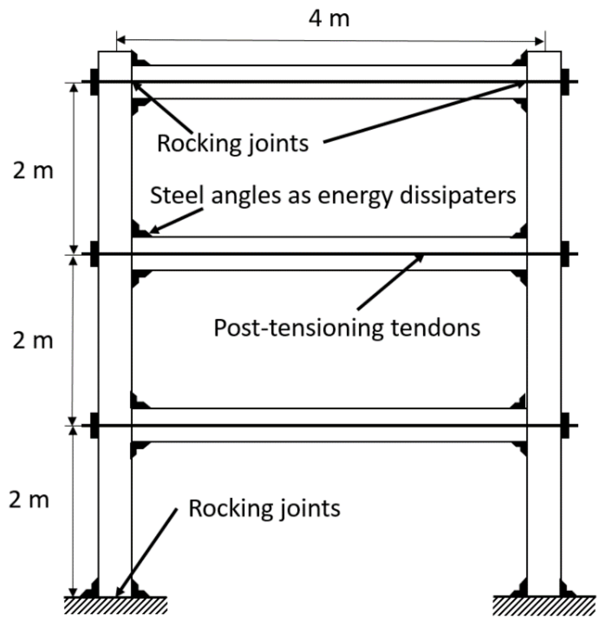

Fig. 6 – 2D multi-storey timber frame

The bay width of the frame is 4 m and the storey height is 2 m. The floor weights are 57.7 kN, 57.7 kN, and 57.3 kN for the first, second, and third storey, respectively. Both column and beam have a cross-section of 320 mm x 200 mm (width x depth). One post-tensioned tendon of 26.5 mm diameter with initial prestressing force of 100 kN is used to tie each beam to the columns at it both ends. The column base is not fixed to the ground, but free to rock. At each beam-column joint, two steel angle plates bolted between the beam and the column face are used as energy dissipating devices. Two steel angle plates are also used at the bottom end of each column to dissipate energy.

In the numerical model, the first storey columns and all beams are modeled with the proposed beam-column elements, with the rocking interface incorporated as an internal rocking hinge based on multispring model. The tendons are each modeled with one single truss element with rigid offset. Each angle dissipating device is modeled with a single spring element incorporated as part of the rocking hinge in the column element. Prestressing forces in the column and tendons are converted as initial deformations in the elements.

The constitutive models the steel angles are the Mander model [23] and Menegotto-Pinto (GMP) model [24] modified by Filippou [25]. Both steel tendon and timber are modeled as linear elastic with the Young's modulus as 170 GPa and 11.1 GPa, respectively. For the steel angles, the stiffness is 10 kN/mm, the yield strength is 12.5 kN, and the hardening ratio 6.7%.

For the internal rocking hinge of the beam-column element, the timber material is modeled with 8 layers of compression-only fibers. The characteristic length is equal to the width of the cross-section. The fundamental periods for the first 3 modes of the numerical model are 0.5 sec, 0.14 sec and 0.07 sec. The input motion is based on a scaled version of the ground motion recorded during the Northridge earthquake from PEER ground motion database. The scaled PGA of this ground motion is 0.3 g.

Fig. 7 shows input ground acceleration, roof displacement time history, and the base shear versus roof displacement relationship. The base shear versus roof displacement relationship has shown a stable flag shape hysteresis loop. These results demonstrate the robust performance of the proposed beam-column element in obtaining structural response.

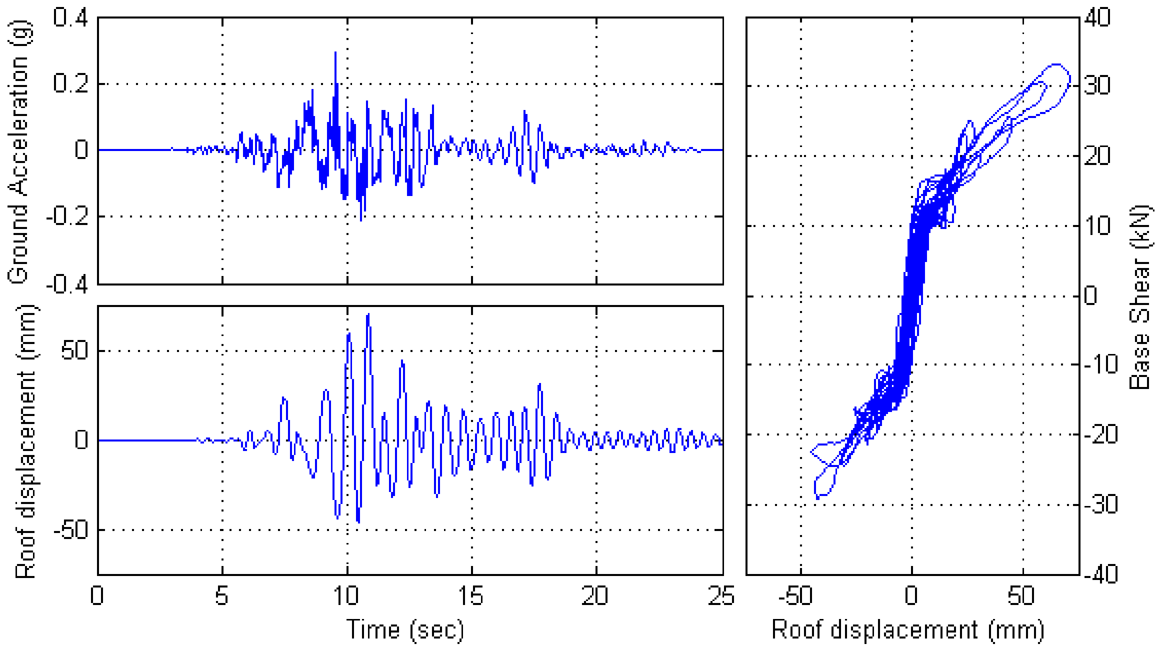

Fig. 7 – Numerical results including roof displacement time history and base shear versus roof displacement relationship

5. Conclusions

In this paper a new beam-column element for modeling rocking members is proposed. It allows rocking joints to be modeled as multispring models within the beam-column element. In addition, this new formulation has the following advantages:

1. Rocking joints can be multiple and at any location within the element, making it favorable for modeling segmental rocking columns.
2. Only the characteristic length of the rocking joint, in addition to the usual material strength parameters, needs to be calibrated against experimental data.
3. The initial flexibility of the whole rocking member prior to gap opening is maintained as exact without the need for any ad-hoc modification of element stiffness.
4. It is applicable to nonlinear inelastic rocking RC beams and columns.
5. No constraint for shear force transfer is needed within the multispring rocking joints.
6. No ill-conditioned stiffness matrix would form.

The accuracy and robust performance of this new beam-column element have been confirmed by comparing numerical results against experimental results for a cantilever rocking RC column subjected to biaxial loading, and in a time history analysis of a 2D multi-storey timber frame subjected to a recorded earthquake ground motion.

6. Acknowledgements

The author thanks Dr. Dion Marriott and Prof. Stefano Pampanin for providing experimental data of the rocking RC column.

7. References

[1] Priestley MN (1991): Overview of presss research program. *PCI Journal*, 36(4), 50–57.

[2] Priestley MN (1996): The presss program current status and proposed plans for phase III. *PCI Journal*, 4(2), 22–40.

[3] Priestley MN, Sritharan S, Conley JR, Pampanin S (1999): Preliminary results and conclusions from the presss five-story precast concrete test building. *PCI Journal*, 44(6), 42–67.

[4] Pampanin S, Priestley MN, Sritharan S (2001): Analytical modelling of the seismic behaviour of precast concrete frames designed with ductile connections. *Journal of Earthquake Engineering*, 5(03), 329–367.

[5] Palermo A, Pampanin S, Calvi GM (2005): Concept and development of hybrid solutions for seismic resistant bridge systems. *Journal of Earthquake Engineering*, 9(06), 899–921.

[6] Kim J (2002): Behavior of hybrid frames under seismic loading. *PhD Thesis*, University of Washington.

[7] Spieth H, Carr A, Murahidy A, Arnolds D, Davies M, Mander J (2004): Modelling of post-tensioned precast reinforced concrete frame structures with rocking beam-column connections. *2004 NZSEE Conference*, Rotoroa, New Zealand.

[8] Palermo A, Pampanin S, Carr A (2005): Efficiency of simplified alternative modelling approaches to predict the seismic response of precast concrete hybrid systems. *Proceedings of fib Symposium "Keep Concrete Attractive"*, Budapest.

[9] Neuenhofer A, Filippou FC (1997): Evaluation of nonlinear frame finite-element models. Jour*nal of Structural Engineering*, 123(7), 958–966.

[10] Lee C-L, Filippou FC (2009): Frame elements with mixed formulation for singular section response. *Int. Journ. Num. Meth. Engrg*, 78(11), 1261–1386.

[11] Marriott D (2009): The Development of High-Performance Post-Tensioned Rocking Systems for the Seismic Design of Structures. *PhD Thesis*, University of Canterbury, Christchurch.

[12] Smith T (2014): Post-tensioned Timber Frames with Supplemental Damping Devices. *PhD Thesis*, University of Canterbury, Christchurch.

[13] Filippou FC, Constantinides M (2004): FEDEASLab getting started guide and simulation examples. *Technical Report NEESgrid-2004-22*, Dept. of Civil and Environmental Eng., University of California at Berkeley.

[14] Mckenna FT (1997): Object-oriented finite element programming: frameworks for analysis, algorithms and parallel computing. *PhD Thesis*, University of California, Berkeley.

[15] Peng BH, Dhakal RP, Fenwick RC, Carr AJ, Bull DK (2013): Multispring hinge element for reinforced concrete frame analysis. *Journal of Structural Engineering*, 139(4), 595–606.

[16] Spacone E, Ciampi V, Filippou FC (1996): Mixed formulation of nonlinear beam finite-element. *Computers & Structures*, 58(1), 71–83.

[17] Taylor RL, Filippou FC, Saritas A, Auricchio F (2003): Mixed finite element method for beam and frame problems. *Computational Mechanics*, 31(1-2), 192–203.

[18] Scott MH, Fenves GL (2006): Plastic hinge integration methods for force-based beam–column elements. *Journal of Structural Engineering*, 132(2), 244–252.

[19] Lee C-L (2008): Hu-Washizu 3d Frame Formulations Including Bond-Slip and Singular Section Response. *PhD Thesis*, University of California, Berkeley.

[20] Lee C-L, Filippou FC (2009): Efficient beam-column element with variable inelastic end zones. *Journal of Structural Engineering*, 135(11), 1310–1319.

[21] Nukala PKVV, White DW (2004): Variationally consistent state determination algorithms for nonlinear mixed beam finite elements. *Computer Methods in Applied Mechanics and Engineering*, 193(33-35), 3647–3666.

[22] Marriott D, Pampanin S, Palermo A (2009): Quasi-static and pseudo-dynamic testing of unbonded post-tensioned rocking bridge piers with external replaceable dissipaters. *Earthquake Engineering & Structural Dynamics*, 38(3), 331–354.

[23] Mander JB, Priestley MJN, Park R (1988): Theoretical stress-strain model for confined concrete. *Journal of Structural Engineering*, 114(8), 1804–1826.

[24] Menegotto M, Pinto PE (1973): Method of analysis for cyclically loaded reinforced concrete plane frames including changes in geometry and non-elastic behavior of elements under combined normal force and bending. *In IABSE*

Symposium on Resistance and Ultimate Deformability of Structures Acted on by Well Defined Repeated Loads, pages 15–22, Lisbon.

[25] Filippou FC, Popov EP, Bertero VV (1983): Effects of bond deterioration on hysteretic behavior of reinforced concrete joints. *Technical Report UCB/EERC-83/19*, Earthquake Engineering Research Center, University of California, Berkeley.

[26] Smith T, Pampanin S, Cesare A, Ponzo F, Simonetti M, Nigro D, Carradine D (2014): Shaking table testing of a multi-storey post-tensioned timber building. In Proc., *Annual Conf. of New Zealand Society for Earthquake Engineering, NZSEE*, Wellington, New Zealand.